Journal of Applied Polymer Science

Miscibility, UV resistance, thermal degradation, and mechanical properties of PMMA/SAN blends and their composites with MWCNTs

Jyotishkumar Parameswaranpillai,[1] George Joseph,[1] Sisanth Krishnan Sidhardhan,[1] Seno Jose,[2] Nishar Hameed[3]

[1]Department of Polymer Science and Rubber Technology, Cochin University of Science and Technology, Cochin, Kerala 682022, India
[2]Department of Chemistry, Government College, Kottayam, Kerala 686013, India
[3]Carbon Nexus, Institute for Frontier Materials, Deakin University, Waurn Ponds Campus, Geelong, VIC 3220, Australia
Correspondence to: J. Parameswaranpillai (E-mail: jyotishkumarp@gmail.com)

ABSTRACT: Poly(methyl methacrylate)/poly(styrene-*co*-acrylonitrile) (PMMA/SAN) blends, with varying concentrations, were prepared by melt-mixing technique. The miscibility is ensured by fixing the acrylonitrile (AN) content of styrene acrylonitrile (SAN) as 25% by weight. The blends were transparent as well. The Fourier transform infrared spectroscopic (FTIR) studies did not reveal any specific interactions, supporting the well accepted 'copolymer repulsion effect' as the driving mechanism for miscibility. Addition of SAN increased the stability of PMMA towards ultraviolet (UV) radiations and thermal degradation. Incorporation of even 0.05% by weight of multi-walled carbon nanotubes (MWCNTs) significantly improved the UV absorbance and thermal stability. Moreover, the composites exhibited good strength and modulus. However, at higher concentrations of MWCNTs (0.5 and 1% by weight) the thermo-mechanical properties experienced deterioration, mainly due to the agglomeration of MWCNTs. It was observed that composites with 0.05% by weight of finely dispersed and well distributed MWCNTs provided excellent protection in most extreme climatic conditions. Thus, PMMA/SAN/MWCNTs composites can act as excellent light screens and may be useful, as cost-effective UV absorbers, in the outdoor applications. © 2016 Wiley Periodicals, Inc. J. Appl. Polym. Sci. **2016**, *133*, 43628.

KEYWORDS: composites; polystyrene; properties and characterization; thermal properties; thermoplastics

Received 6 July 2015; accepted 14 March 2016
DOI: 10.1002/app.43628

INTRODUCTION

Polymer blending has been evolved as a promising, cost-effective method, mainly due to the scope of maximal diversification and increased use of existing polymers, to accomplish remarkable broad spectrum of properties. Based on the miscibility between the component polymers, polymer blends are classified into immiscible, partially miscible, and completely miscible blends. Poly(methyl methacrylate) (PMMA) is an important candidate for commercial glass products. Because of its good thermo-mechanical properties and high transparency in the visible region, it has been widely applied in aircraft glazing, signs and displays, lens for glasses, lamp covers, indicators, etc. Styrene acrylonitrile (SAN) offers superior mechanical properties, chemical resistance, and thermal stability in comparison with polystyrene (PS) and is widely used in place of PS for various end use applications including packaging, electronic, medical, and automotive applications.

It is unequivocally established that poly(methyl methacrylate)/poly(styrene-*co*-acrylonitrile) (PMMA/SAN) blends are miscible, if the acrylonitrile (AN) content in the SAN is below 30%.[1–23] Note that PMMA is neither miscible with polystyrene (PS) nor with polyacrylonitrile (PAN). For most miscible polymer pairs, there must be a favorable enthalpic driving force, as the entropic contribution is very small due to the high molecular masses of the components of the mixture.[12] However, PMMA is miscible with SAN due to the so called 'copolymer repulsion effect' between S and AN segments of the copolymer. Although the term 'repulsion effect' is a misnomer, studies have shown that in blends, where at least one component is a random copolymer, miscibility does not always need favorable interactions between the component chains, the necessary negative value of the Flory–Huggins interaction parameter, χ, can be achieved from the 'copolymer repulsion effect'. For this blend, the interaction energy density may be given as:

$$B = B_{S-MMA}\phi_1 + B_{MMA-AN}\phi_2 - B_{S-AN}\phi_1\phi_2$$

where $B_{S\text{-}MMA}$, $B_{MMA\text{-}AN}$, and $B_{S\text{-}AN}$ are the binary interaction parameters of styrene (S), methacrylate (MMA), and acrylonitrile (AN), respectively, and ϕ_1 and ϕ_2 are the volume fractions of component polymers in the blend.[9,12] It is obvious from this equation that B may become negative even if all interaction

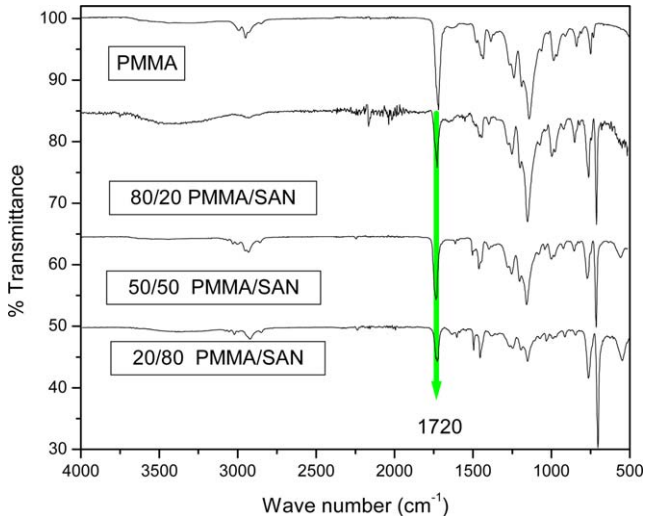

Figure 1. FTIR spectra of PMMA and PMMA/SAN blends. [Color figure can be viewed in the online issue, which is available at wileyonlinelibrary.com.]

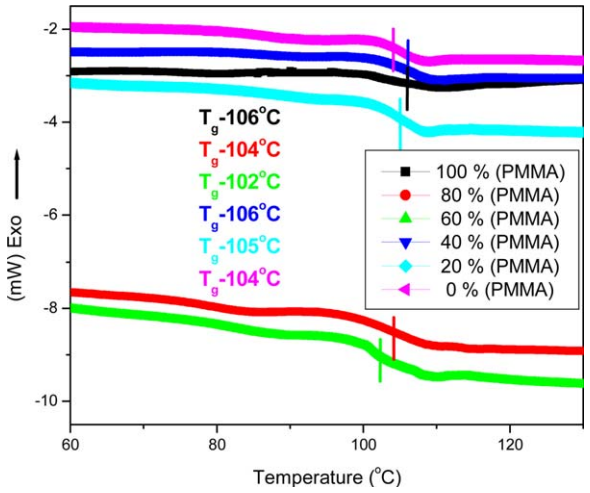

Figure 2. Effect of blend ratio on the glass transition temperature (T_g) of the PMMA/SAN blends. [Color figure can be viewed in the online issue, which is available at wileyonlinelibrary.com.]

parameters are positive (which is true for PMMA/SAN blends), when the repulsive interactions between S and AN in SAN is greater than the sum of the repulsive interactions between S and MMA and AN and MMA. It is important to recognize that specific inter-chain interactions, responsible for molecular compatibility of dissimilar polymers, tend locally to align the chain segments for association and thus stiffen the chains, and reduce their convolution, resulting in reduced entanglement between dissimilar chains.[10]

The miscibility of PMMA/SAN blends was studied in detail by using various experimental techniques such as optical and torsional pendulum measurements,[2] cloud point measurements,[1,5,7,9] small angle neutron scattering (SANS),[6,13] differential scanning calorimetry (DSC),[14,18] rheology,[17,20] atomic force microscopy (AFM),[19] positron life time measurements,[21] and small angle light scattering (SALS).[22,23] Most of these studies support 'copolymer repulsion mechanism' as the driving force for miscibility, while a few researchers reported on the specific attractive interactions between carbonyl groups of PMMA and phenyl groups of SAN.[4,15]

Table I. Characteristic Group Frequencies Observed in FTIR Spectra of PMMA and PMMA/SAN Blends[26–30]

Peak (cm^{-1})	Remarks
699	Benzene ring C=C out-of plane bending of SAN
1145	C-O-C stretching of ester group of PMMA
1188	
1237	
1270	
1215, 1650	C-C non-saturated bonds
1400–1500	Aromatic C=C absorption in SAN
1720	C=O stretching of MMA
2850	C-H symmetric stretching

A few studies have been reported on the phase separation of PMMA/SAN blends in the presence of nanoparticles.[24,25] Yu and coworkers[24,25] have studied the effect of silica nanoparticles on the phase separation of these blends, using rheological methods and optical microscopy, and found that a small amount of silica nanoparticles significantly altered the phase diagram of the blends. Although PMMA/SAN blends are extensively studied, no systematic study has been published related to the thermo-mechanical and ultraviolet (UV) resistance properties of the PMMA/SAN blend. Therefore, the prime objective of the present study is to explore the thermal degradation, UV resistance, and tensile properties of these blends and their composites with multi-walled carbon nanotubes (MWCNTs). To ensure complete miscibility between the SAN and PMMA phase, we have taken SAN copolymer with 25% of acrylonitrile content. Fourier transform infrared spectroscopy (FTIR), differential scanning calorimetry (DSC), UV spectrometry, high-resolution transmission electron microscopy (HRTEM), thermogravimetric analysis (TGA), and tensile test were used to characterize and evaluate the properties of the blends.

EXPERIMENTAL

Materials

Poly(methyl methacrylate) (PMMA), grade PERSPEX® CP-61 with a density of 1.18 g/cm^3, was supplied by Plaskolite West (Compton, CA, USA). Poly(styrene-*co*-acrylonitrile) (SAN), LG SAN 82TR with a density of 1.07 g/cm^3, was supplied by LG Chem. Pvt. The SAN contained around 75% styrene and 25% acrylonitrile. The MWCNTs, synthesized by catalytic carbon vapor disposition process (purity > 95%, average diameter 13–16 nm, and length > 1 μm) (Baytube VR 150P), were supplied by Bayer Material Science AG (Leverkusen, Germany).

Preparation of Blends and Composites

PMMA/SAN blends were prepared by melt-mixing, using Thermo Haake Polylab QC system equipped with roller rotors. The mixing was done at 180 °C with a rotor speed of 60 rpm for 15 min. Among the prepared PMMA/SAN blends, 80/20

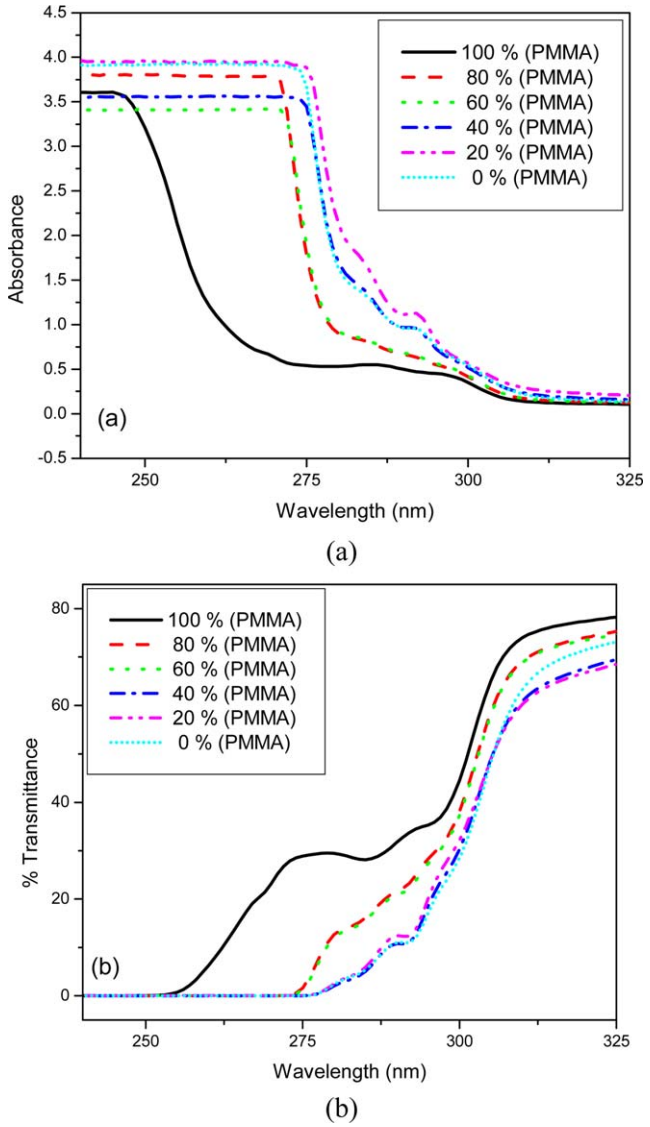

Figure 3. Ultraviolet (a) absorption and (b) transmission spectra of PMMA, SAN, and their blends. [Color figure can be viewed in the online issue, which is available at wileyonlinelibrary.com.]

blends possess the best properties, in terms of strength and elongation; therefore these blends were taken as the matrix for composites. For making PMMA/SAN (80/20)/MWCNTs composites, PMMA and SAN were pre-mixed and melt-mixed for 5 min, followed by the addition of MWCNTs. The concentrations of MWCNTs used were 0.05, 0.1, 0.5, and 1% by weight. The mixing was continued for 10 more minutes at 180 °C and 60 rpm. The resulting blends and composites were hot pressed at 180 °C using a hydraulic press (model SHP-50, Zeus controls Pvt., India), at a pressure of 200 kg/cm^2 into sheets and cut into pieces and compression molded at 200 °C at a pressure of 200 kg/cm^2, for preparing test specimens.

Characterization

FTIR Spectroscopy. Infrared studies were conducted to investigate the interaction between the blend components. The samples were scanned from 4000 to 400 cm^{-1}, using a FTIR-8400S spectrophotometer (Shimadzu).

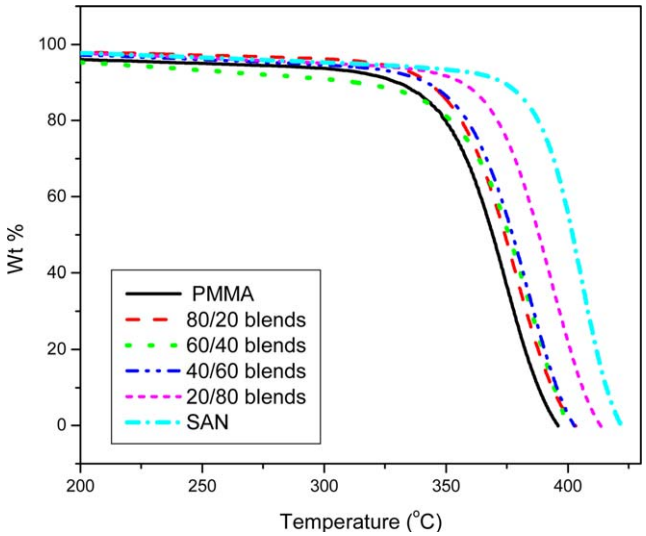

Figure 4. Thermogravimetric curves of PMMA, SAN, and their blends. [Color figure can be viewed in the online issue, which is available at wileyonlinelibrary.com.]

Differential Scanning Calorimetry. The glass transition temperatures (T_g) of PMMA/SAN blends were determined using a Mettler Toledo DSC 822e. The measurements were performed using 2-10 mg of the samples, in nitrogen atmosphere, at a heating and cooling rates of 10 °C min^{-1}, in the temperature range of 40–160 °C.

UV Spectrophotometry. The UV absorbance and transmittance studies were conducted using a Cary 5000 spectrometer (Varian). The blend samples were scanned from 175–400 nm, with a wavelength accuracy of ± 0.1 nm.

Transmission Electron Microscopy (TEM). High-resolution transmission electron micrographs of the nanocomposites were taken with a JEOL JEM 2100 transmission electron microscope (TEM), with an accelerating voltage of 200 kV. Ultrathin sections of bulk specimens (100 nm thickness) were prepared at room temperature, using an ultra-microtome fitted with a diamond knife.

Thermogravimetric Analysis. Thermal stability of PMMA/SAN blends was analyzed by using a thermogravimetric analyzer

Table II. Initial Decomposition Temperature (T_i), Maximum Decomposition Temperature (T_{max}), and Activation Energy for Decomposition (E_a) of PMMA, SAN, and Their Blends

Sample	(T_i) (°C)	T_{max} (°C)	E_a (kJ/mol)
PMMA	338	370	70.6
80/20 blends	344	375	73.5
60/40 blends	350	382	77.2
40/60 blends	352	385	84.3
20/80 blends	367	392	88.9
SAN	387	406	119.8

Table III. Weight Percentage of PMMA/SAN Blends Remained at Different Temperatures

Temperature (°C)	PMMA	80/20 blends	60/40 blends	40/60 blends	20/80 blends	SAN
100	99	99	99	99	99	99
200	96	98	95	97	98	98
300	94	96	91	95	95	95
350	80	86	81	86	92	93
375	37	48	49	52	73	89
390	7	16	16	19	44	77
395	1	8	7	9	32	68

(TGA), Perkin Elmer, Diamond TG/DTA. The measurements were performed using 5-10 mg of the samples, in the temperature interval from 25 to 700 °C, at a heating rate of 20 °C min^{-1}, in nitrogen atmosphere.

Tensile Testing. Tensile measurements were performed according to ASTM D-882 standards. The measurements were taken with a universal testing machine (Tinius Olsen), Model H 50 KT, at a crosshead speed of 10 mm min^{-1}. Rectangular specimens of 80 × 10 × 0.5 mm^3 were used for determining the tensile strength. The tests were performed on six different specimens of the same sample and the average was taken as the final value.

RESULTS AND DISCUSSION

PMMA/SAN Blends

FTIR Spectroscopy. As mentioned previously, it is widely accepted that the mechanism of miscibility of PMMA/SAN blends is due to 'copolymer repulsion effect' even if there are reports that miscibility is due to the specific interactions between the carbonyl group (C = O) of PMMA and phenyl group or hydrogen of SAN. In this study, we carried out the IR absorption measurements to detect the possible interactions between SAN and PMMA. FTIR spectra and characteristic group frequencies observed in the spectra are given in Figure 1 and Table I, respectively. It should be noted that favorable interactions between C = O group of PMMA and phenyl or H of SAN would have resulted in a significant shift in the C = O stretching frequency of PMMA at 1720 cm^{-1}. Further, C-O-C stretching frequencies of ester groups of PMMA, observed in between 1145 and 1270 cm^{-1}, might have changed. However, IR spectra revealed that there is no significant change in these peaks. The possibility of strong intermolecular interactions, such as hydrogen bonding or dipole interactions, which may lead to the miscibility of the certain polymer systems, can be neglected as there is no significant shift in the corresponding absorption peaks of the groups, which are involved in those interactions. However, the peaks of aromatic C = C absorption in the spectrum of SAN are observed at 1400–1500 cm^{-1}. Thus, the FTIR study supported the absence of any favorable specific interactions between the PMMA and SAN, which in turn supports the so called 'copolymer repulsion effect' as the driving force of miscibility of PMMA with SAN.

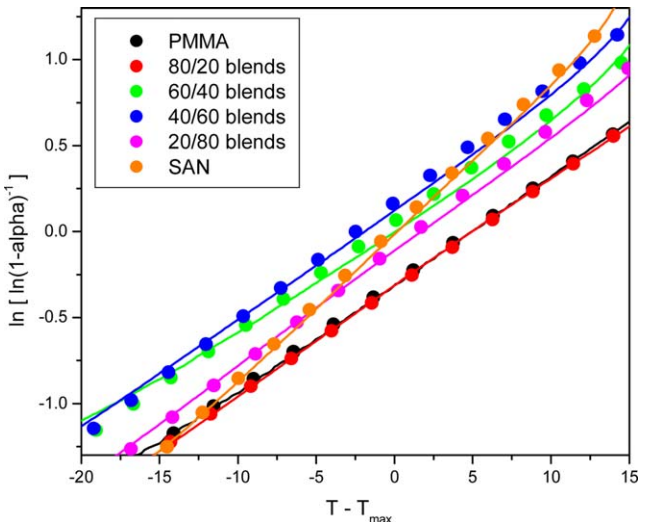

Figure 5. Arrhenius plots for the activation energy for the decomposition (E_a) of PMMA, SAN, and their blends. [Color figure can be viewed in the online issue, which is available at wileyonlinelibrary.com.]

Differential Scanning Calorimetry. Differential scanning calorimetry (DSC) is one of the most widely used techniques to characterize the miscibility level of polymer blends. The criterion for miscibility, most frequently used in polymer blends, is the appearance of a single glass transition (T_g) in the blend at a temperature intermediate between those of the pure components. However, in the case of PMMA/SAN blends, since the T_g's of the pure components are close to each other (106 and 104 °C, respectively, for PMMA and SAN), in an experimental DSC thermogram, it is difficult to distinguish between two overlapped transitions, and a single one broader than those of the pure components. Song *et al.*[14] have shown that modulated differential scanning calorimetry can be used to resolve the glass transitions of PMMA/SAN miscible blends. Cameron *et al.*[18] studied the temperature dependence of the relaxation times of miscible PMMA/SAN blends with different AN contents, by modeling DSC thermograms obtained after different thermal histories in each sample. They observed homogeneity in PMMA/SAN blends, where AN content of SAN is close to the upper limit of miscibility. Thus, in the present case, display of a single T_g in that range (Figure 2) cannot be taken as a direct evidence of miscibility. Although this barrier could be overcome by conducting DSC thermograms on samples previously subjected to different thermal treatments, it is beyond the scope of the present study.

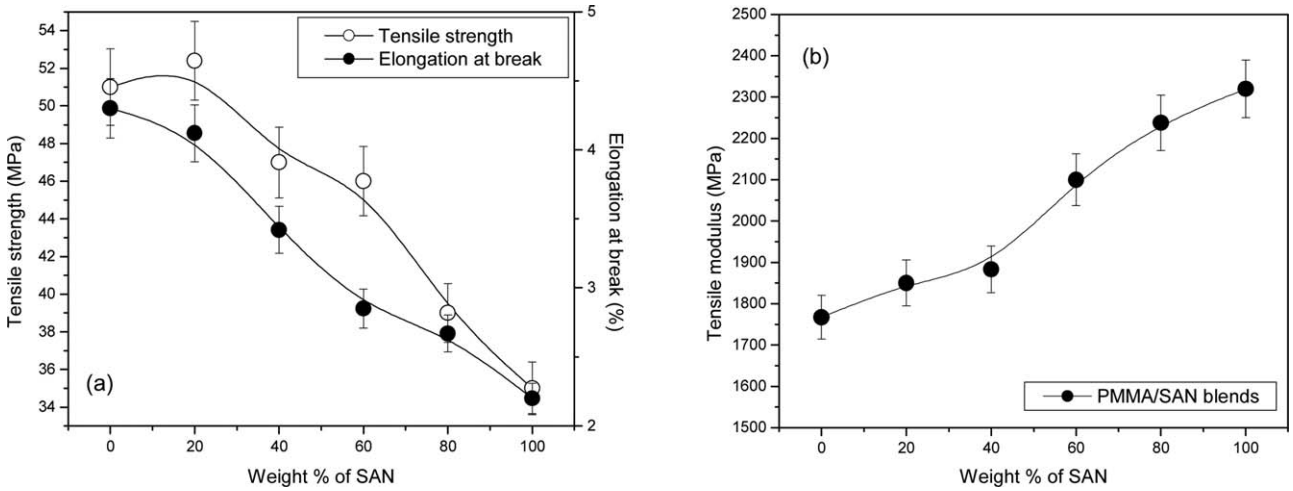

Figure 6. Tensile properties of the PMMA/SAN blends: (a) tensile strength and elongation at break; and (b) tensile modulus.

UV Absorbance and Transmittance. To evaluate the optical properties of the blends, the UV absorption and transmission spectra were taken and are shown in Figure 3(a,b). From the UV profile, it is quite clear that PMMA filters ultraviolet light at wavelengths below 250 nm. It may be attributed to the n-π* transition of C = O group present in PMMA.[31,32] However, SAN filters ultraviolet light at wavelengths below 280 nm. The addition of SAN into PMMA improves the absorption to 275 nm range and hence ultraviolet-C light can be effectively shielded. It is interesting to note that addition of 20% by weight of SAN (80/20 blends) remarkably enhances the absorption of UV radiations by the sample. Further addition has not considerable impact on the percentage absorbance. It is obvious from the figure that UV shielding efficiency of the samples enhances with the increase in the amount of SAN in the blends. The transmittance of the UV radiation through the blends is less compared to neat PMMA samples. In other words, PMMA/SAN blends have higher shielding efficiency than the neat PMMA, such that the blends absorb UV light below 275 nm, which is very harmful to human health (for example, the skin and eyes are most sensitive to damage by UV below 275 nm) and can be screened.

Thermogravimetric Analysis. Thermal stability of PMMA/SAN blends was studied by thermogravimetric analyzer (TGA) in nitrogen atmosphere. TGA curves for the blends are given in Figure 4. The thermal stability of the blends is higher than that of neat PMMA. Thermal stability can be expressed in terms of parameters like initial decomposition temperature (T_i), where the sample starts degradation, and maximum decomposition temperature (T_{max}), where the rate of degradation is the fastest. T_i and T_{max}, obtained from the thermogram are given in Table II. From the thermograms and table, it is clear that T_i and T_{max} increase with the increase in the concentration of SAN in the blends and a maximum was obtained for the neat SAN system. Table III, which shows the effect of blend ratio on the weight percentage of the sample at seven selected temperatures, gives a clear picture about extent of improvement in the thermal stability achieved by the addition of SAN into PMMA.

For a better understanding of the thermal stability of the blends, activation energy was calculated using the Horowitz-Metzger equation given by

$$\ln[\ln(1-\alpha)^{-1}] = E_a\theta/RT_{max}^2 \quad (1)$$

where α is the decomposed fraction, E_a is the activation energy for decomposition, T_{max} is the temperature at maximum rate of weight loss, R is the universal gas constant, and θ is given by $T - T_{max}$. The E_a is calculated from the slope of the plot of $\ln[\ln(1-\alpha)^{-1}]$ against θ. Figure 5 shows the Arrhenius plots for the E_a for the decomposition of PMMA and SAN in PMMA/SAN blends. The effect of blend ratio on the E_a of PMMA/SAN blend is shown in Table II. E_a of PMMA and SAN are found to be 70.6 and 119.8 kJ mol^{-1}, respectively. It is seen that addition of SAN into PMMA increases the E_a of blends. Since the blend is homogeneous, we have only one E_a. Attention should be paid to the fact that an increase in E_a indicates that more energy is

Table IV. Relative Tensile Strength and Adhesion Parameters of PMMA Rich Blends

PMMA/SAN Blend	σ_b/σ_p	S	S′	K_b
90/10	0.88	0.99	1.15	0.51
80/20	1.03	1.31	1.61	−0.08
70/30	0.95	1.4	1.80	0.10
60/40	0.93	1.61	2.13	0.13
50/50	0.87	1.83	2.49	0.20
Mean	0.93	1.42	1.82	0.18

Table V. Relative Tensile Strength and Adhesion Parameters of SAN Rich Blends

PMMA/SAN Blend	σ_b/σ_p	S	S′	K_b
10/90	0.93	1.02	1.17	0.35
20/80	1.09	1.34	1.62	−0.29
30/70	1.09	1.51	1.91	−0.21
40/60	1.31	2.10	2.4	−0.60
50/50	1.26	2.40	3.22	−0.42
Mean	1.14	1.68	2.14	−0.24

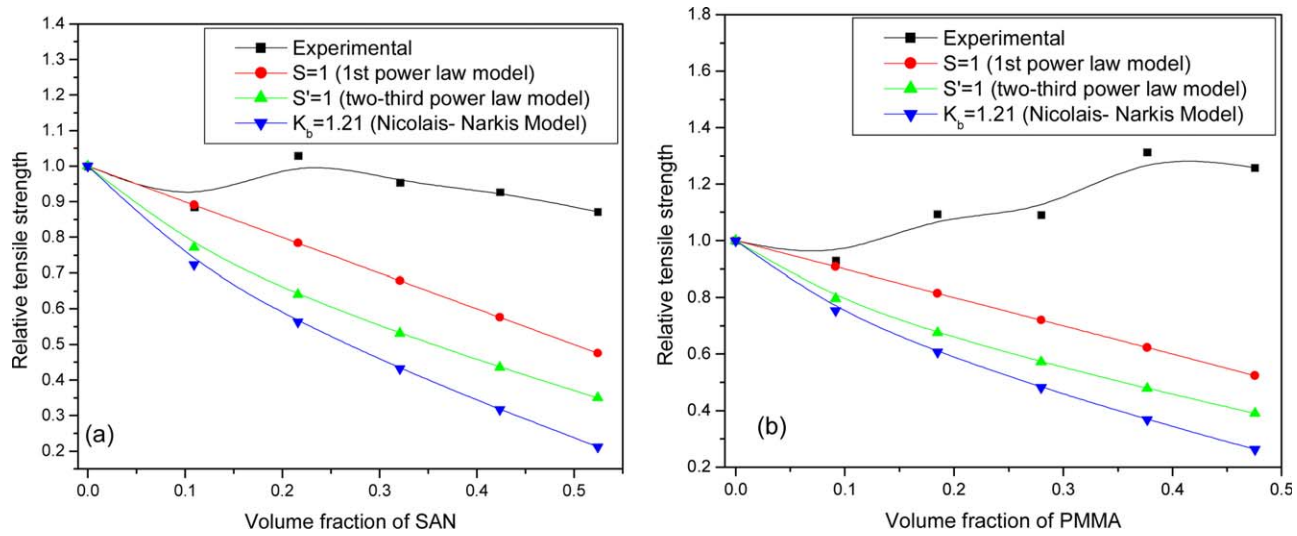

Figure 7. Plot of relative tensile strength versus volume fraction of (a) PMMA rich blends and (b) SAN rich blends. [Color figure can be viewed in the online issue, which is available at wileyonlinelibrary.com.]

required for the major degradation step, which in turn implies an improvement in thermal stability of the blends. Thus, it can be concluded that as the amount of SAN in the blend increases, the thermal stability also increases.

Tensile Properties. Tensile properties of the blends are shown in Figure 6(a,b). It is observed that the tensile strength and elongation at break decrease with the increase in the concentration of SAN in the blends, due to the inherent brittle nature of the SAN phase. However, addition of SAN into the blends increases the modulus. Among the various blends, 80/20 blends possess the best properties, in terms of strength and elongation.

Theoretical Modeling. Theoretical analysis of tensile strength. In order to understand the level of interaction between the component polymers in PMMA/SAN blends, predictive models were used to tensile strength data. These models include:

Nielsen's first power law model[33]:

$$\frac{\sigma_b}{\sigma_p} = (1-\phi_1)S \tag{2}$$

Nielsen's two-third power law model[33]:

$$\frac{\sigma_b}{\sigma_p} = \left(1-\phi_1^{2/3}\right)S' \tag{3}$$

Nicolais-Narkis model[34]:

$$\frac{\sigma_b}{\sigma_p} = \left(1-K_b\phi_1^{2/3}\right) \tag{4}$$

where σ_b and σ_p represent the tensile strength of the blend and the major component of the blend, respectively, ϕ_1 is the volume fraction of the minor phase, S and S′ are Nielsen's parameters in the first and two-third power law models, respectively, and K_b is an adhesion parameter. S and S′ account for the weakness in the structure, brought about by the discontinuity

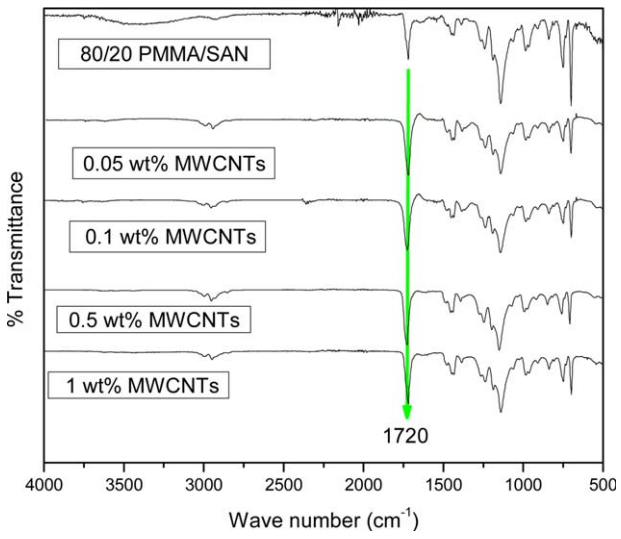

Figure 8. FTIR spectra of PMMA/SAN (80/20) blends and PMMA/SAN (80/20)/MWCNTs composites. [Color figure can be viewed in the online issue, which is available at wileyonlinelibrary.com.]

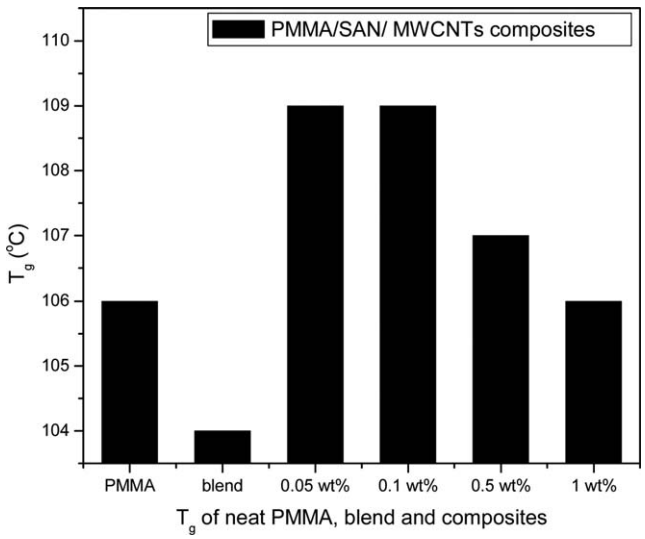

Figure 9. Glass transition temperature (T_g) of PMMA, PMMA/SAN (80/20) blends, and PMMA/SAN (80/20)/MWCNTs composites.

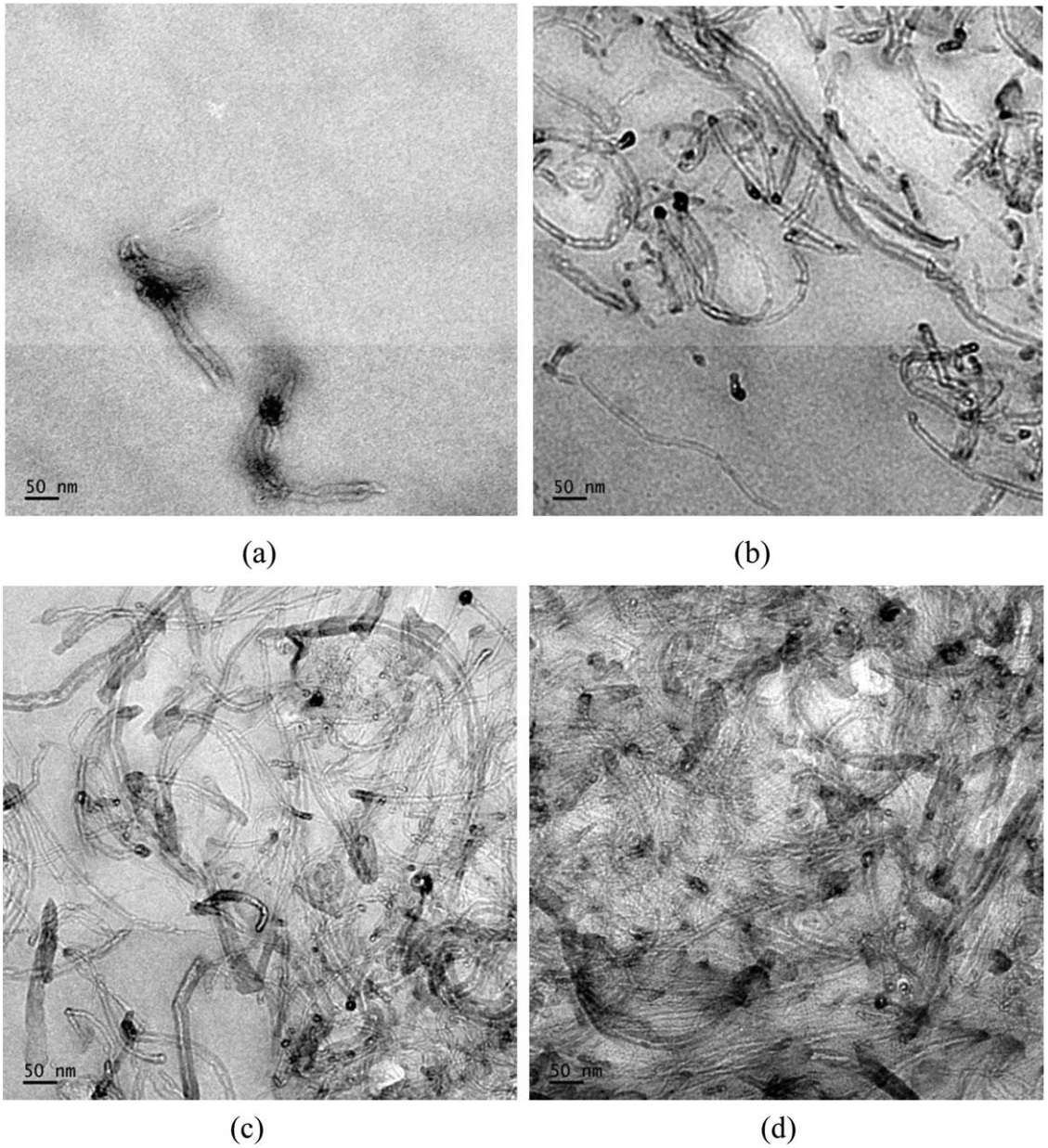

Figure 10. TEM images of PMMA/SAN(80/20)/MWCNTs composites (a) 0.05 wt % MWCNTs, (b) 0.1 wt % MWCNTs, (c) 0.5 wt % MWCNTs, and (d) 1 wt % MWCNTs.

in stress transfer and generation of the stress concentration at the interfaces in the case of blends. The values of S and S′ are unity if there is no stress concentration effect. The value of K_b is 1.21 for spherical inclusions of the minor phase, having no adhesions. Although these models are proposed for filled polymer systems and are used in immiscible polymer blends to inspect the level of interfacial adhesion in the absence of compatibilizer,[35,36] we apply these models in PMMA/SAN miscible blends to get an idea about the extent of deviation resulting from the miscible nature of the system. The values of relative tensile strength (σ_b/σ_p), S, S′, and K_b are listed in Tables IV and V. From the tables, it is obvious that the values of S and S′ are greater than unity suggesting good adhesion between the blend components. Further, the values of K_b are too small or even negative indicating perfect adhesion between the blend components.

Plots of relative tensile strength versus volume fraction of the blends, predicted using the three models, are presented in Figure 7. From Figure 7(a), it is obvious that in all the blends, where PMMA forms the major phase, the experimental data are far away from that predicted by the models. In other words, the experimental relative tensile strength values are far better than those of the models. This means that there exists strong interactions between the blend components or the blends are completely miscible. Note that in the present case, the miscibility is not due to favorable interactions. Figure 7(b) shows that for SAN rich blends also the experimental data are far better than

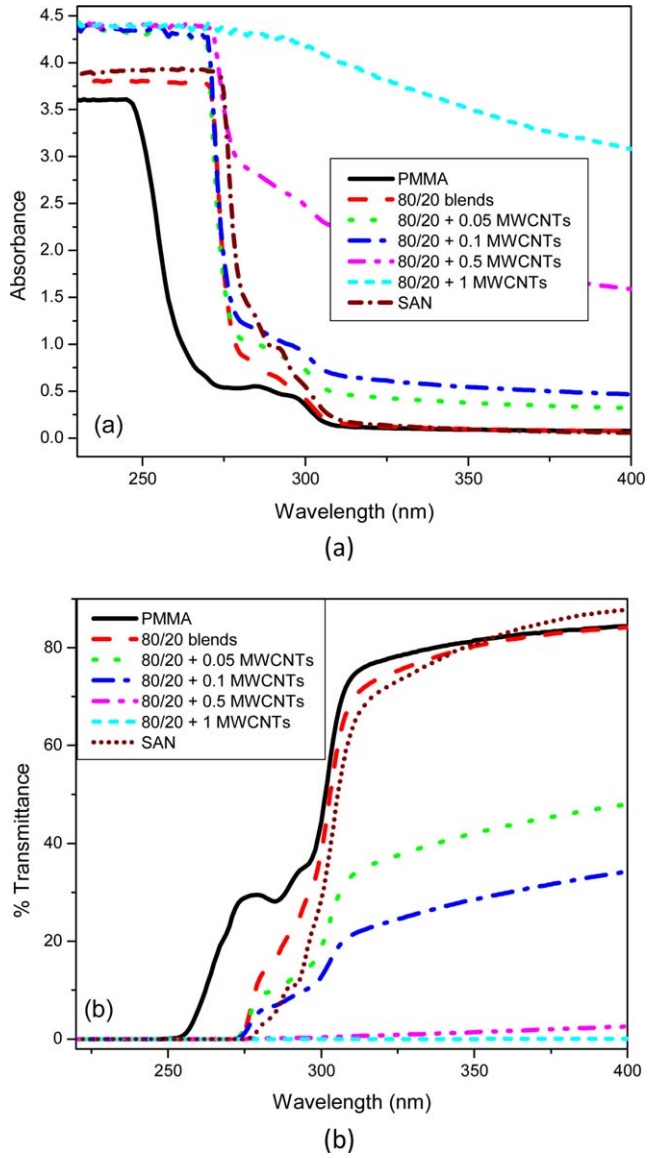

Figure 11. Ultraviolet (a) absorbance and (b) transmittance spectra of PMMA, SAN, PMMA/SAN (80/20) blends, and PMMA/SAN (80/20)/MWCNTs composites. [Color figure can be viewed in the online issue, which is available at wileyonlinelibrary.com.]

those predicted by models. This means that when SAN forms the matrix, there is greater adhesion between the two components in the blend. Nielsen's two-third power law model and Nicolais-Narkis model deviate from the experimental results. Nielsen's first power law model suggests that there is good compatibility between the blend components only when the concentration of SAN is $\leq$10% by weight. In short, these models failed to explain the experimental data, mainly due to the completely miscible nature of the component polymers.

PMMA/SAN (80/20)/MWCNTs Composites

FTIR Spectroscopy. FTIR studies were performed to detect any possible interactions between MWCNTs and polymers. We observed no significant change in the characteristics peaks of various groups obtained for the composites (Figure 8) and PMMA/SAN blends (Figure 1). This means that the presence of MWCNTs in the blends has no impact on the miscibility of PMMA/SAN blends. This is not unexpected as the driving force for the miscibility of the blends is the 'copolymer repulsion effect' and not any specific exothermic interactions, which give rise to a negative enthalpy of mixing.

Differential Scanning Calorimetry. The T_g values for various composite systems are given in Figure 9. The presence of MWCNTs, up to 0.1% by weight in the blends, increases the T_g of PMMA/SAN blends by 5 °C (from 104 to 109 °C). This does not mean that there is strong interaction between the blends and MWCNTs, which was already ruled out by FTIR studies. Note that the glass transition process is related to the molecular

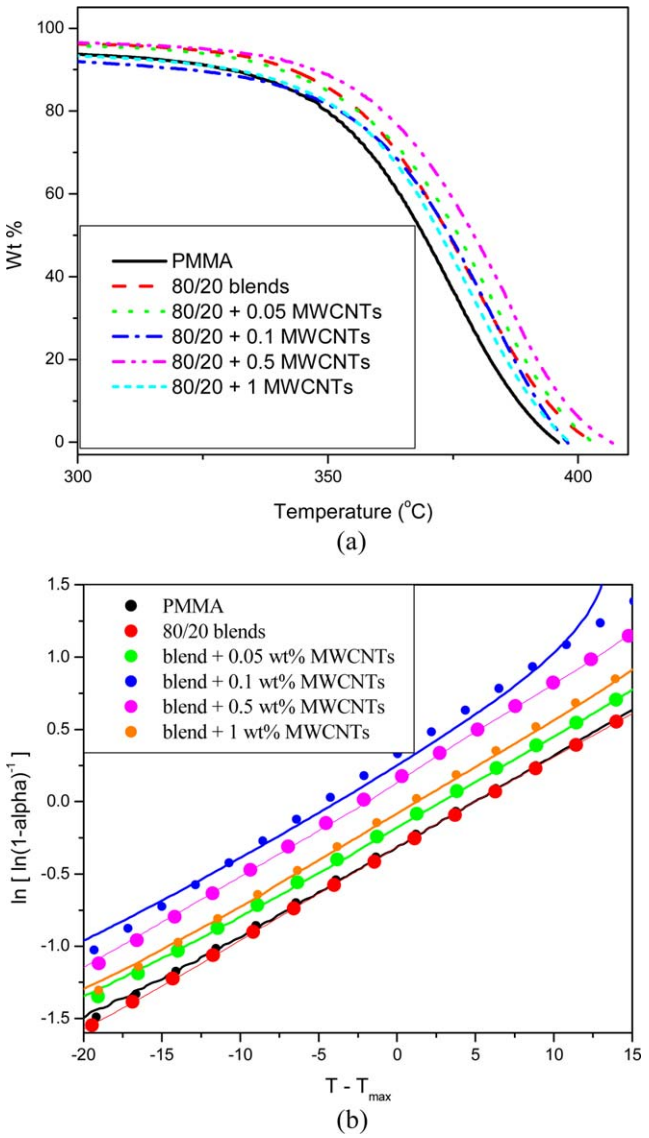

Figure 12. (a) Thermogravimetric curves of PMMA, PMMA/SAN (80/20) blends, and PMMA/SAN (80/20)/MWCNTs composites. (b) Arrhenius plots for the activation energy for the decomposition of PMMA, PMMA/SAN (80/20) blends, and PMMA/SAN (80/20)/MWCNTs composites. [Color figure can be viewed in the online issue, which is available at wileyonlinelibrary.com.]

Table VI. T_i, T_{max}, and E_a of PMMA, PMMA/SAN (80/20) Blends, and PMMA/SAN (80/20)/MWCNTs Composites

Sample	(T_i) (°C)	T_{max} (°C)	E_a (kJ/mol)
PMMA	338	370	70.6
80/20 blends	344	375	73.5
80/20 blends + 0.05 wt % MWCNTs	355	379	74.2
80/20 blends + 0.1 wt % MWCNTs	353	384	86
80/20 blends + 0.5 wt % MWCNTs	356	385	82.7
80/20 blends + 1 wt % MWCNTs	352	377	77.3

motion. Hence, molecular packing, chain rigidity, entanglements, and linearity affect the T_g. Increase in T_g of the composites in comparison to that of neat blend may be attributed to the adhesion between the blends and the MWCNTs, where the nanometer sized MWCNTs can slightly restrict the segmental motion of PMMA/SAN polymer chains. However, beyond 0.1% by weight of MWCNTs, the dispersion may be poor due to weak van der Waals force of attraction between the CNTs, which eventually leads to their agglomeration and deterioration of properties of composites.

The High-Resolution Transmission Electron Microscope (HRTEM) Images. TEM images of composites are shown in the Figure 10. It is seen that for composites containing 0.05% by weight of MWCNTs, the nanotubes are well dispersed in the polymer matrix. However, as the concentration of MWCNTs in the blend increases, MWCNTs tend to stick to each other, which they love to do, due to van der Waals' interactions, resulting agglomeration.

UV Absorbance and Transmittance. From Figure 11(a,b), it is seen that MWCNTs effectively filter the UV radiations. Even at lower concentration of MWCNTs (for example, at 0.05 wt % of MWCNTs), the composites could effectively screen the high-energy UV radiations. Note that PMMA/SAN/0.05 wt % of MWCNT composites possess greater UV absorbance than neat SAN, even beyond 300 nm. This, in turn, indicates that nanotubes are well dispersed in the polymer matrix. It is worth emphasizing that the percentage transmittance of UV radiation through the composites decreases from 80 to 40% with the addition of 0.05% by weight of MWCNTs. Presence of 0.1% by weight of MWCNTs in the composites further reduces the percentage transmittance. Although at higher concentrations of the filler (for example, at 1% by weight of MWCNTs), the percentage transmittance of UV radiations through the composites decreases to zero for the entire UV range in the spectrum, and the transparency of the sample is diminished. Previous studies have shown that nanoparticles strongly absorb UV – VIS radiations[37] and reduce the transmittance properties of composites as they act as strong scattering centers[38,39] The percentage reduction of transmittance with the addition of nanoparticles may be attributed to the formation of small crystalline domains.[38] In short, PMMA/SAN/MWCNTs composite, with even 0.05 wt % of finely dispersed and well distributed MWCNTs, can effectively shield UV radiations and act as excellent light screen and UV absorber. Thus, it is concluded PMMA/SAN/MWCNTs composites can provide excellent protection against most extreme climatic conditions and will be cost effective for making lightweight UV shields.

Thermogravimetric Analysis. T_i, T_{max}, and E_a obtained from the thermograms of the composites (Figure 12) are shown in Table VI. From the table, it is obvious that the thermal stability

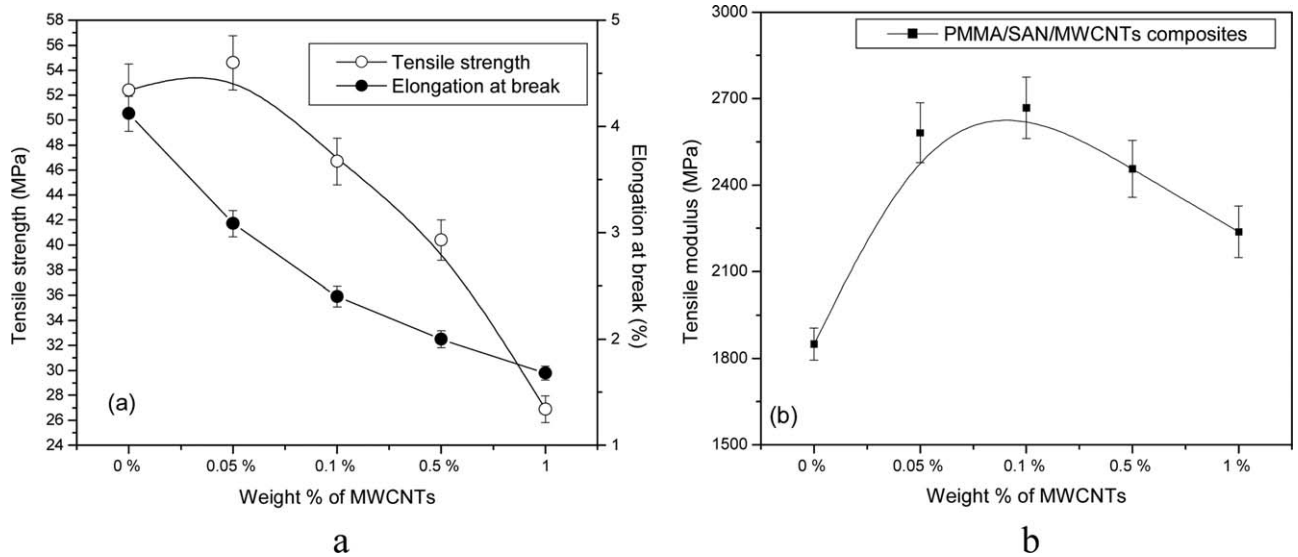

Figure 13. Tensile properties of the PMMA/SAN/MWCNTs composites (a) tensile strength and elongation at break (b) tensile modulus.

of the composites increases in the presence of MWCNTs. In our previous publications, we reported that incorporation of nanofillers only marginally improve the thermal stability of immiscible and incompatible multiphase systems.[40,41] However, in the present case, a considerable enhancement in thermal stability is observed by the addition of even 0.1% by weight of MWCNTs. T_i and T_{max} increase by 9 °C, whereas E_a by ca. 15%. The significant improvement in thermal stability may be due to the finely dispersed and uniformly distributed nanoparticles in miscible systems. However, in immiscible systems, nanoparticles prefer to stay at the interface or may preferentially be dispersed in one of the phases. It is important to note that at higher concentrations of MWCNTs viz. 0.5 and 1% by weight of MWCNTs, there is marginal decrease in the thermal stability. This may be attributed to the increase in rate of agglomeration of nanoparticles at high concentrations.

Tensile Properties. Figure 13 shows mechanical properties of various MWCNTs reinforced composites. Tensile strength and modulus increase on the addition of MWCNTs. Tensile strength is maximum for composites containing only 0.05% by weight of MWCNTs, while Young's modulus is maximum for composites with 0.1% by weight of MWCNTs. Elongation at break, on the other hand decreases with increase in concentration of MWCNTs. From the FTIR spectra, it is clear that there are no favorable specific interactions between polymer matrix and MWCNTs. Hence, the increase in tensile strength and modulus may be attributed to the reinforcing effect of MWCNTs on the matrix, due to the interfacial adhesion between polymer matrix and nanofillers. Various researchers reported on the mechanical properties of polymer nanocomposites reinforced with CNTs and have shown that CNTs are excellent reinforcing agents for polymer matrices.[42–48] Spitalsky *et al.*[42] extensively reviewed the mechanical properties of CNT based polymer nanocomposites. Effects of addition of various types of CNTs on the mechanical properties of the epoxy matrix have been reviewed by Domun *et al.*[43] However, many of the studies revealed that incorporation of high filler loading might diminish mechanical properties, due to particle agglomeration.[47,48] However, upon increasing the concentration of MWCNTs, tensile properties decrease due to agglomeration of MWCNTs.

CONCLUSIONS

This article is devoted to investigate the miscibility, UV absorbance, thermal degradation, and tensile properties of PMMA/SAN blends and their composites with MWCNTs. FTIR studies revealed that the miscibility of PMMA/SAN blends is not due to favorable specific interactions between PMMA and SAN polymer chains and supported the widely accepted 'copolymer repulsion mechanism'. MWCNTs acted as excellent nanofillers for PMMA/SAN system as their addition remarkably reduced UV transmittance, improved thermal stability, and modulus of PMMA/SAN blends. The glass transition temperatures (T_g's) of PMMA and SAN are so close that DSC analysis could not distinguish the T_g's of individual polymers. The presence of MWCNTs marginally increased the T_g of the blends. UV absorption and transmission spectra disclosed that PMMA/SAN blends have higher shielding efficiency than the neat PMMA and the presence of SAN reduced transmittance of UV radiations. It was observed that incorporation of MWCNTs could effectively filter UV radiations because the finely dispersed and uniformly distributed MWCNTs in the composites could effectively shield the high-energy UV radiations. High-resolution TEM images revealed that MWCNTs are well dispersed in polymer matrix only at very low concentration of the filler and higher concentrations of the filler facilitate the agglomeration of CNTs. It was also found that the addition of SAN into PMMA significantly improved the thermal stability of the blends and the presence of 0.1% by weight of MWCNTs appreciably enhanced the thermal stability of the systems. At high filler concentrations (>0.1% by weight), a marginal decrement in thermal stability is observed due to the agglomeration of nanofillers. In addition, the presence of MWCNTs at very low concentrations reinforced PMMA/SAN system, in terms of tensile strength and modulus. In short, PMMA/SAN/MWCNTs composites can act as an excellent light screens and may be useful as ultraviolet (UV) shields in outdoor applications, including automotive applications as they exhibit good strength and modulus coupled with excellent thermal stability.

ACKNOWLEDGMENTS

J.P. acknowledges the Department of Science and Technology, Government of India, for financial support under an Innovation in Science Pursuit for Inspired Research (INSPIRE) Faculty Award (contract grant number IFA-CH-16). N.H. acknowledges funding from VESKI under the Victoria Fellowship. S.J. acknowledges the University Grants Commission, Government of India, for financial assistance for undertaking minor research project in sciences.

REFERENCES

1. McMaster, L. P. *Macromolecules* **1973**, *6*, 760.
2. Stein, V. D. J.; Jung, R. H.; Illers, K.-H.; Hendus, H. *Macromol. Mater. Eng.* **1974**, *36*, 89.
3. Bernstein, R. E.; Cruz, C. A.; Paul, D. R.; Barlow, J. W. *Macromolecules* **1977**, *10*, 681.
4. Naito, K.; Johnson, G. E.; Allara, D. L.; Kwei, T. K. *Macromolecules* **1978**, *11*, 1260.
5. Schmitt, B. J. *Angew. Chem. Int. Engl. Edn.* **1979**, *18*, 273.
6. Schmitt, B. J.; Kirste, R. G.; Jelenic, J. *Makromol. Chem.* **1980**, *181*, 1655.
7. Kressler, J.; Kammer, H. W.; Klostermann, K. *Polym. Bull.* **1986**, *15*, 113.
8. Fowler, M. E.; Barlow, J. W.; Paul, D. R. *Polymer* **1987**, *28*, 2145.
9. Suess, M.; Kressler, J.; Kammer, H. W. *Polymer* **1987**, *28*, 957.
10. Wu, S. *Polymer* **1987**, *28*, 1144.
11. Cowie, J. M. G.; Lath, D. *Makromol. Chem. Macromol. Symp.* **1988**, *16*, 103.
12. Nishimoto, M.; Keskkula, H.; Paul, D. R. *Polymer* **1989**, *30*, 1279.

13. Hahn, K.; Schmitt, B. J.; Kirschey, M.; Kirste, R. G.; Salie, H.; Strecker, S. S. *Polymer* **1992**, *33*, 5150.
14. Song, M.; Hammiche, A.; Pollock, H. M.; Hourston, D. J.; Reading, M. *Polymer* **1995**, *36*, 3313.
15. Feng, H.; Ye, C.; Feng, Z. *Polym. J.* **1996**, *28*, 661.
16. Robertson, C. G.; Wilkes, G. L. *Polymer* **2001**, *42*, 1581.
17. Zheng, Q.; Du, M.; Yang, B.; Wu, G. *Polymer* **2001**, *42*, 5743.
18. Cameron, N.; Cowie, J. M. G.; Ferguson, R.; Gomez Ribelles, J. L.; Mas Estelles, J. *Eur. Polym. J.* **2002**, *38*, 597.
19. Wen, G.; Li, X.; Liao, Y.; An, L. *Polymer* **2003**, *44*, 4035.
20. Du, M.; Gong, J.; Zheng, Q. *Polymer* **2004**, *45*, 6725.
21. Kumaraswamy, G. N.; Ranganathaiah, C.; Urs, M. V. D.; Ravikumar, H. B. *Eur. Polym. J.* **2006**, *42*, 2655.
22. Prusty, M.; Keestra, B. J.; Goossens, J. G. P.; Anderson, P. D. *Chem. Eng. Sci.* **2007**, *62*, 1825.
23. Keestra, B. J.; Goossens, J. G. P.; Anderson, P. D. *Chem. Eng. Sci.* **2011**, *66*, 4960.
24. Gao, J.; Huang, C.; Wang, N.; Yu, W.; Zhou, C. *Polymer* **2012**, *53*, 1772.
25. Huang, C.; Gao, J.; Yu, W.; Zhou, C. *Macromolecules* **2012**, *45*, 8420.
26. Feng, H.; Shen, L.; Feng, Z. *Eur. Polym. J.* **1995**, *31*, 243.
27. Torikai, A.; Hiraga, S.; Fueki, K. *Polym. Degrad. Stabil.* **1992**, *37*, 73.
28. Colom, X.; Garcia, T.; Sunol, J. J.; Saurina, J.; Carasco, F. *J. Non-Cryst. Sol.* **2001**, *287*, 308.
29. Xia, Q.; Zhao, X. J.; Chen, S. J.; Ma, W. Z.; Zhang, J.; Wang, X. L. *eXPRESS Polym. Lett.* **2010**, *4*, 284.
30. Gong, X.; Kozbiala, A.; Li, L. *Chem. Sci.* **2015**, *6*, 3478.
31. Chiantore, O.; Trossarelli, L.; Lazzari, M. *Polymer* **2000**, *41*, 1657.
32. Wu, X.; Wang, Y.; Zhu, P.; Sun, R.; Yu, S.; Du, R. *Mater. Lett.* **2011**, *65*, 705.
33. Nielsen, L. E. *J. Appl. Polym. Sci.* **1966**, *10*, 97.
34. Nicolais, L.; Narkis, M. *Polym. Eng. Sci.* **1971**, *11*, 194.
35. Jose, S.; Nair, S. V.; Thomas, S.; Karger-Kocsis, J. *J. Appl. Polym. Sci.* **2006**, *99*, 2640.
36. Parameswaranpillai, J.; Joseph, G.; Jose, S.; Hameed, N. *J. Appl. Polym. Sci.* **2015**, *132*, 42100. DOI: 10.1002/app.42100
37. Zhang, L.; Gong, X.; Bao, Y.; Zhao, Y.; Xi, M.; Jiang, C.; Fong, H. *Langmuir* **2012**, *28*, 14433.
38. Reyes-Acosta, M. A.; Torres-Huerta, A. M.; Domínguez-Crespo, M. A.; Flores-Vela, A. I.; Dorantes-Rosales, H. J.; Ramírez-Meneses, E. *J. Alloys Comp.* **2015**, *643*, S150.
39. Lee, S.; Shin, H.-J.; Yoon, S.-M.; Yi, D. K.; Choi, J.-Y.; Paik, U. *J. Mater. Chem.* **2008**, *18*, 1751.
40. Parameswaranpillai, J.; Joseph, G.; Shinu, K. P.; Jose, S.; Salim, N. V.; Hameed, N. *RSC Adv.* **2015**, *5*, 25634.
41. Parameswaranpillai, J.; Joseph, G.; Shinu, K. P.; Sreejesh, P. R.; Jose, S.; Salim, N. V.; Hameed, N. *Mater. Chem. Phys.* **2015**, *163*, 182.
42. Spitalsky, Z.; Tasis, D.; Papagelis, K.; Galiotis, C. *Prog. Polym. Sci.* **2010**, *35*, 357.
43. Domun, N.; Hadavinia, H.; Zhang, T.; Sainsbury, T.; Liaghat, G. H.; Vahida, S. *Nanoscale* **2015**, *7*, 10294.
44. Mallakpour, S.; Madani, M. *J. Appl. Polym. Sci.* **2015**, *132*, DOI: 10.1002/app.42022.
45. Roy, S.; Srivastava, S. K.; Pionteck, J.; Mittal, V. *Macromol. Mater. Eng.* **2015**, *300*, 346.
46. Dadfar, S. M. M.; Kavoosi, G. *Polym. Compos.* **2015**, *36*, 145.
47. Wegrzyn, M.; Sahuquillo, O.; Benedito, A.; Gimenez, E. *J. Appl. Polym. Sci.* **2015**, *132*, DOI: 10.1002/app.42014.
48. George, N.; Chandra, C. S. J.; Mathiazhagan, A.; Joseph, R. *Compos. Sci. Technol.* **2015**, *116*, 33.